CrossMark

ORIGINAL ARTICLE

Callosal anatomical and effective connectivity between primary motor cortices predicts visually cued bimanual temporal coordination performance

Mathias Wahl[1] · Birgit Lauterbach-Soon[1] · Elke Hattingen[3] · Annemarie Hübers[1,4] · Ulf Ziemann[1,2]

Abstract Default in-phase coupling of hand movements needs to be suppressed when temporal coordination is required for out-of-phase bimanual movements. There is lack of knowledge on how the brain overrides these default in-phase movements to enable a required interval of activity between hands. We used a visually cued bimanual temporal coordination (vc-BTC) paradigm with a constant rhythmical time base of 1 s, to test the accuracy of in-phase and out-of-phase (0.1, 0.2,…,0.9) finger tapping. We hypothesized that (1) stronger anatomical and effective interhemispheric connectivity between the hand areas of the primary motor cortex (M1$_{HAND}$) predict higher temporal offsets between hands in the out-of-phase conditions of the vc-BTC; (2) patients with relapsing-remitting multiple sclerosis (RRMS) and clinically isolated syndrome (CIS) have reduced interhemispheric connectivity and altered between-hand coupling. Anatomical connectivity was determined by fractional anisotropy of callosal hand motor fibers (FA-hCMF). Effective connectivity was probed by short interval interhemispheric inhibition (S-IHI) using paired-coil transcranial magnetic stimulation (TMS). In healthy subjects, higher FA-hCMF and S-IHI correlated with higher temporal offsets between hands in the out-of-phase conditions of the tapping test. FA-hCMF was reduced in patients with RRMS but not in CIS, while S-IHI was reduced in both patient groups. These abnormalities were associated with smaller temporal offsets between hands leading to less deviation from the required phasing in the out-of-phase tapping conditions. Findings provide multiple levels of evidence that callosal anatomical and effective connectivity between the hand areas of the motor cortices play important roles in visually cued bimanual temporal coordination performance.

Abbreviations

CC	Corpus callosum
CMF	Callosal motor fibers
CIS	Clinically isolated syndrome
DTI	Diffusion tensor imaging
EDSS	Expanded disability status scale
FA	Fractional anisotropy
FA-hCMF	Fractional anisotropy of hand callosal motor fibers
FDI	First dorsal interosseous
hCMF	Hand callosal motor fibers
M1$_{HAND}$	Primary motor cortex hand area
MEP	Motor evoked potential
9-HPT	Nine-hole peg test
NAWM	Normal appearing with matter
RMT	Resting motor threshold
RRMS	Relapsing-remitting multiple sclerosis
S-IHI	Short interval interhemispheric inhibition

✉ Ulf Ziemann
ulf.ziemann@uni-tuebingen.de

1 Department of Neurology, Goethe University, Frankfurt, Germany

2 Department of Neurology and Stroke, and Hertie Institute for Clinical Brain Research, Eberhard-Karls University, Hoppe-Seyler-Str. 3, 72076 Tübingen, Germany

3 Institute of Neuroradiology, Goethe University, Frankfurt, Germany

4 Present Address: Department of Neurology, University Clinic, Ulm, Germany

TMS   Transcranial magnetic stimulation
vc-BTC   Visually cued bimanual temporal
            coordination

Introduction

The motor system generates an impressing variety of spatially and temporally coordinated bimanual movements enabling humans to interact with their environment in a meaningful way. However, while the temporal and spatial constraints effective in bimanual coordination have been quite extensively studied on a behavioral level, little is known about the neurophysiological and microstructural determinants underlying bimanual temporal coordination (BTC). Previous work has demonstrated that two intrinsic phase-locked conditions, "in-phase" and "anti-phase" are preferred in BTC. Early experiments, in which healthy subjects were requested to reproduce various initially externally cued out-of-phase tapping conditions from memory (one movement cycle per second), showed a tendency for out-of-phase conditions (offset between hands, 0.1–0.4 s or 0.6–0.9 s) to drift into neighboring in-phase or anti-phase tapping (Yamanishi et al. 1980). Therefore, when environmentally specified instructions require meaningful intermanual timing, these intrinsically preferred movement patterns need to be suppressed. In the presence of an external pacer, attraction to in-phase movements is not apparent (Tuller and Kelso 1989) and healthy subjects deviate away from in-phase movements at externally cued out-of-phase conditions indicating that the motor system engages an effective mechanism to suppress in-phase oscillators. In patients with callosotomy, however, strong attraction to in-phase movements even in the presence of an external pacer has been demonstrated, suggesting that the ability to generate out of phase BTC patterns depends on the integrity of the corpus callosum (Tuller and Kelso 1989). Even though a large body of evidence exists, that the motor corpus callosum plays a pivotal role in this context (Jeeves et al. 1988; Serrien et al. 2001; Tuller and Kelso 1989), disclosure of its specific nature and function has only started recently. This became possible with the advent of imaging and electrophysiological techniques which can precisely and directly relate structural connectivity or effective connectivity to behavior (Johansen-Berg et al. 2007; Hübers et al. 2008). Likewise, effective connectivity as referred to the influence that one neural system exerts over another (Friston et al. 1993), either at a synaptic or population level, can be assessed by modern imaging and electrophysiological techniques and specifically linked with aspects of motor behavior (Hübers et al. 2008).

Variation of white matter microstructural features in the body of the CC predicted variation in the performance of a bimanual coordination task (Johansen-Berg et al. 2007). We showed, that short interval interhemispheric inhibition (S-IHI), a marker of effective connectivity between the primary motor cortex hand areas ($M1_{HAND}$) of the two hemispheres (Ferbert et al. 1992) correlated inversely with the amount of electromyographic (EMG) mirror activity in a hand muscle during intended unimanual movements (Hübers et al. 2008). Here, we employed for the first time a tri-modal experimental design of testing the relation of BTC performance, as measured by an established visually cued finger tapping paradigm (Tuller and Kelso 1989), with anatomical and effective connectivity, as measured by fractional anisotropy (FA) of interhemispheric motor pathways (hand callosal motor fibers, hCMFs), a marker of microstructural fiber pathway integrity (Pierpaoli et al. 1996; Basser and Pierpaoli 1996), and S-IHI, respectively. We built this study on our previous experiments, where we demonstrated a significant relation between FA-hCMFs and S-IHI between $M1_{HAND}$ in healthy subjects (Wahl et al. 2007).

We hypothesized that anatomical connectivity (FA-hCMF) and effective connectivity (S-IHI) between $M1_{HAND}$ of the two hemispheres predict the degree of between-hand temporal offsets in vc-BTC performance of healthy subjects. In addition, we tested patients with relapsing-remitting multiple sclerosis (RRMS) in the identical BTC protocol. We chose multiple sclerosis as a model disease of callosal damage, given the findings of frequent and early callosal affection in RRMS (Evangelou et al. 2000a, b; Pelletier et al. 2001; Zito et al. 2014). We have shown previously, that impaired S-IHI along with reduced FA-hCMF is already present in the earliest stages of RRMS (Wahl et al. 2011), but the behavioral implications of these findings have not been tested. We tested here the hypothesis that relative to healthy controls MS patients show reduced between-hand offsets due to reduced anatomical and effective interhemispheric connectivity.

Materials and methods

Subjects

Twelve healthy subjects (mean age 32.6 ± 9.0 years, range 26–51 years, 5 females) and 22 early stage RRMS patients or clinically isolated syndrome (CIS) patients [mean age 31.9 ± 6.0 years, range 22–45 years, mean disease duration 17.3 ± 14.0 months, 15 females, median EDSS 1.5 (range 0–2.0)] were included in this study. FA and S-IHI data of the healthy subjects have been reported earlier (Wahl et al. 2007, 2011). Among the patients, 7 were diagnosed with CIS, and 15 had RRMS, according to the revised McDonald criteria (Polman et al. 2011).

Concerning the RRMS group, 11 patients had participated and their S-IHI and FA-hCMF data had been reported already in our previous study (Wahl et al. 2011). Written informed consent was obtained from all subjects prior to participation. The study conformed to the latest revision of the Declaration of Helsinki and was approved by the ethics committee of the medical faculty of the Goethe-University of Frankfurt/Main. Inclusion criteria were as follows: age ≥18 years, right-handedness as determined by the Edinburgh Handedness Inventory (Oldfield 1971), and for patients: EDSS ≤2.0. In addition, although formally not an inclusion criterion, all patients had a normal central motor conduction time of ≤9.0 ms to the first dorsal interosseous (FDI) muscle of both hands. Exclusion criteria for transcranial magnetic stimulation (TMS) were adopted from Rossi et al. (2009). For MRI, the locally (Brain Imaging Center, Goethe University Frankfurt/Main) defined exclusion criteria were applied (i.e., the presence of pacemakers, defibrillators, neurostimulators, artificial heart valves, implants or prostheses which are not MR compatible, cochlear implants, acupuncture needles, insulin or pain pumps, metal splinters or any metal parts (plates, screws, wires) in the body, artificial joints, larger tattoos or tattoos with metal powder). Finally, a history of optic neuritis and/ or a delayed P100 latency of the visually evoked potential were defined as exclusion criteria for participation in the vc-BTC task because these instances are expected to be associated with alterations of visual information processing, while we were interested specifically in alterations in the interhemispheric motor aspects of this task. Therefore, 6/15 RRMS patients and 2/7 CIS patients were excluded. In addition, 2 RRMS patients reported problems with concentration, fatigue and blurred vision while performing vc-BTC task, which led to their discontinuation of the task.

All experimental data of a given participant (one imaging session for measuring FA-hCMF, one session for testing of S-IHI and vc-BTC performance) were always obtained within 14 days.

Image acquisition

MRI was acquired in a 3-Tesla Magnetom Trio (Siemens Medical Solutions, Erlangen, Germany) as described earlier (Wahl et al. 2007, 2011). Structural T1-weighted images were acquired with a magnetization-prepared rapid-acquisition gradient echo (MPRAGE) sequence [repetition time (TR) 2250 ms, echo time (TE) 26 ms, inversion time 900 ms, flip angle 9°, 192 sagittal slices, field of view 256 × 256 mm, voxel size 1 × 1 × 1 mm]. Fluid-attenuated inversion recovery (FLAIR) images [repetition time (TR) 6000 ms, echo time (TE) 353 ms, inversion time (TI) 2200 ms, sagittal slices, voxel size 1 × 1 × 1 mm] were also acquired. For bihemispheric identification of $M1_{HAND}$,

fMRI was performed in a block design experiment using BOLD-sensitive echo planar imaging (EPI) (TR 2640 ms, TE 30 ms, flip angle 90°, 36 transverse slices, 0.75 mm gap, voxel size 3 × 3 × 3 mm, base resolution 64 × 64). Online EPI distortion correction was done as described by others (Zaitsev et al. 2004). Subjects performed a visually instructed simple motor task that consisted of index finger tapping at a self-paced rate of ∼2 Hz, while a total of 192 scans were acquired. DTI data were acquired with a single shot spin-echo EPI with parallel imaging technique GRAPPA (generalized auto-calibrating partially parallel acquisitions, acceleration factor 2) with the following parameters: 12 gradient directions, b value of 700, TR 7200 ms, TE 80 ms, voxel size 1.9 × 2.0 × 1.9 mm, 60 transverse slices, base resolution 128 × 128.

FMRI analysis

For processing of fMRI data, Brain Voyager (Brain Innovation, The Netherlands) was used. For data preprocessing, interslice scan time correction with sinc interpolation and three-dimensional (3D) motion correction was performed. During fMRI data post-processing, the automated motion correction also provided a plot that showed the translation and rotation shifts on over time. Relevant motion artifacts were considered if the translations in the x-, y- and/or z-axes exceeded 2 mm, or if the rotations along the x-, y- and/or z-axes exceeded 2°.

No relevant motion artifacts were detected. Temporal filtering of the realigned time series was performed using a high-pass filter of three data points, before linear drifts of the signal were eliminated from each pixel's time course. Alignment of fMRI and 3D anatomical data included an initial automatic header-based alignment before manual fine tuning was done to adjust rotational and translational parameters. Time course correlation of the measured BOLD signal with a hemodynamic reference function was performed at each voxel in order to acquire a correlation coefficient r. After thresholding at 80 % of the maximum correlation coefficient in $M1_{HAND}$, the resulting functional area was applied to the anatomical data set as overlay. We exported the anatomical data set with the overlaid (unchangeable) functional areas as DICOM files.

Registration of different datasets

We used the commercial BrainLAB® planning software package iPlan®. This software uses normalized mutual information-based registration as image similarity measures to register the fMRI-overlayed anatomical images with the DTI images (Pluim et al. 2003). The mutual information algorithms measured only those parts of the reference image containing the participant's head, whereas

the program detected and excluded background regions and potential non-anatomical objects before registration. The normalized mutual information finds image similarities by feature-based image alignment algorithm, using T1w MPRAGE as the reference and DTI data set as sensed or floated images. The method finds correspondence between image features such as edges, contours, surfaces, other salient features such as corners, line intersections, and points of high curvature, statistical features such as moment invariants, and higher-level structural descriptions. Knowing the correspondence between a number of points in images, a geometrical transformation is then determined to map the target image to the reference images, thereby establishing point-by-point correspondence between the reference and target images. The program also takes into account the registration problem resulting from different resolutions of the floating images compared to the reference anatomical data, since DTI images have a larger voxel size and slice thickness. To avoid artificial maxima to mutual information, lowpass-filtering smoothed the coarse-scaled DTI data before subsampling. On a coarse scale, mutual information should have a broad maximum at the correct transformation and the optimization method should converge to this maximum from a large set of initial states. The registration algorithms were semi-automatic, so that we could verify the correctness of a registration. In case of insufficient results, we restricted the region of interest and repeated registration algorithms to increase the accuracy (PatXfer 5.1, BrainLab, image fusion software module) (Nimsky et al. 2006).

Fiber tracking

We performed fiber tracking on the preregistered multimodal data sets. The tracking algorithm implemented in BrainLAB© was based on a local diffusion approach with deterministic fiber tracking. Mori et al. first published the underlying Fiber Assignment by Continuous Tracking (FACT) algorithm (Mori and van Zijl 2002). To get smooth results despite of the low resolution of normal DTI scans, the tensors were interpolated from the surrounding voxels, a method which is called Tensor Deflection (TEND) (Nimsky et al. 2006; Lazar et al. 2003; Weinstein et al. 1999). The major eigenvector of each seed was calculated and bidirectional iteration was initiated until one of the stop criteria FA <0.15 or deviation angle >40° was met. Tractography was initiated from a rectangular region of interest (ROI) that covered M1$_{HAND}$ defined by fMRI in the right and left hemisphere to visualize corticofugal fibers originating from M1. In all cases, this first tracking step exhibited a majority of fibers descending through the internal capsule, but a small number of fibers crossing the corpus callosum were also detectable. Therefore, in a

further step, a smaller rectangular ROI was adjusted to the area of the CC that exhibited fibers after the first tracking step and bidirectional tractography was repeated. Only those tracked fibers projecting into or near to the functionally defined left and right M1$_{HAND}$ were retained, including at least one more voxel beyond the gray/white matter boundary. This means that the final tracking result only included fiber tracts projecting from the CC into the M1$_{HAND}$ of both hemispheres (cf. Wahl et al. 2007).

DTI quantification

Mean FA was calculated for hand CMFs from all voxels within the boundaries of the CC rather than from the entire CMF pathway avoiding contamination from crossing fibers, which are absent within the midbody of the CC. A distance of one voxel to the CC/CSF boundary (indicated by FA <0.4) was respected to avoid inclusion of partial volumes of surrounding CSF.

Short interval interhemispheric inhibition (S-IHI)

S-IHI from the left M1$_{HAND}$ to the right M1$_{HAND}$ was studied, using paired-coil TMS (Ferbert et al. 1992). We chose this direction, as we showed previously that S-IHI in healthy right-handers was expressed more consistently from the left to right hemisphere than vice versa (Netz et al. 1995). TMS was delivered through two Magstim 200 magnetic stimulators with a monophasic current waveform (The Magstim Company, UK) connected to figure-of-eight coils (inner diameter of each loop, 70 mm). The conditioning coil was placed tangentially over the left M1$_{HAND}$ with the handle pointing laterally. The test coil was placed over the right M1$_{HAND}$, with the handle pointing backwards and 45° away from the midline. For both coils, the optimal position was determined as the site eliciting consistently, at a slightly suprathreshold intensity, the largest motor evoked potentials (MEPs) in the FDI of the contralateral hand. The resting motor threshold (RMT) was determined for the conditioning pulse to the nearest 1 % of maximum stimulator output using the relative frequency method (Groppa et al. 2012), and was defined as the minimum stimulus intensity that resulted in small MEPs >50 µV in at least five of ten trials. To obtain a wide range of S-IHI magnitudes from threshold to maximum, the intensity of the conditioning stimulus (CS) was scaled from 100 to 150 % RMT in 10 % steps (i.e., six different intensities). The intensity of the test pulse was adjusted to produce an unconditioned mean MEP of 1 mV in peak-to-peak amplitude. S-IHI was tested at an interstimulus interval of 12 ms. S-IHI testing comprised of eight trials per CS intensity and eight unconditioned test stimulus trials (i.e., total of 56 trials) that were applied in randomized

order in a single block of trials. To reduce anticipation of the next trial, the intertrial interval was randomly varied between 4 and 6 s. Conditional averages of the single trial MEP peak-to-peak amplitudes were calculated. For each CS intensity, S-IHI was expressed by $(1 -$ mean conditioned MEP/mean unconditioned MEP$) \times 100$ %. Accordingly, IHI $= 100$, 0 and <0 % indicate complete interhemispheric inhibition, no effect and interhemispheric facilitation, respectively. To obtain one single value of S-IHI for correlation analyses with vc-BTC and FA-hCMF, for each participant the mean S-IHI over the CS intensities of 130–150 % RMT was calculated. These intensities were selected because our previous study in healthy subjects had demonstrated correlations selectively in this high-intensity range of S-IHI with FA-hCMF (Wahl et al. 2007).

For determination of S-IHI, MEPs were recorded from the FDI of both hands by surface EMG using bipolar Ag–AgCl cup electrodes mounted on the FDI motor point and the proximal phalanx of the index finger. The S-IHI measurements were obtained during muscle rest. Involuntary FDI activation was monitored by audio-visual feedback of the high-gain (50 µV/Division) EMG raw signal. Trials contaminated by muscle activation (<1 % of all trials) were discarded from further analysis. This is important as previous studies showed that muscle activation alters S-IHI (Ferbert et al. 1992; Nelson et al. 2009). The EMG was bandpass filtered (20 Hz to 2 kHz) and amplified (Counterpoint Mk2 Electromyograph, Dantec, Denmark), digitized at a sampling rate of 4 kHz per channel (CED Micro 1401; Cambridge Electronic Design, UK), and stored on a computer for offline analysis. Customized Spike2 software (Cambridge Electronic Design) was used for experimental control, data acquisition and online and offline data analysis.

Visually cued bimanual temporal coordination (vc-BTC) performance

The task used here was selected for the following reasons: (1) patients with callosotomy perform bimanual synchronous finger tapping normally but show deficits with asynchronous finger tapping, indicating that asynchronous finger tapping depends on the integrity of the CC (Tuller and Kelso 1989); (2) it has been shown in a stepwise callosotomy case study, that the posterior CC is necessary especially for bimanual coordination timing in response to external cues (Eliassen et al. 2000). Since the task selected here also probes externally cued bimanual temporal coordination, it is perfectly integrated into the framework of our hypothesis because the system under investigation (hand CMFs) is localized in the posterior part of the CC (Hofer and Frahm 2006; Zarei et al. 2006; Meyer et al. 1995; Wahl et al. 2007; Fling et al. 2013).

Vc-BTC was tested in all healthy subjects and a subset of 12 patients (5 CIS and 7 RRMS) using an established finger tapping protocol (Tuller and Kelso 1989). We expected that MS patients would show similar impairment of vc-BTC as patients with callosotomy, in particular if FA or S-IHI revealed callosal disconnection. Subjects sat in a chair with their shoulders adducted, elbows flexed at $\sim 90°$ and forearms and hands resting on armrests in a pronated position. Wrists were taped to the armrests so that index finger tapping movements were restricted to the metacarpophalangeal joint. A uni-axial accelerometer (Model 2256A-100; voltage sensitivity, 100 mV/g; Endevco Corp., USA) was fixed at the dorsum of the proximal phalange of the index finger of either hand to record index finger movements in the extension–flexion axis. Subjects faced the modified front view of an I/O board (CED Micro 1401), which displayed a central fixation point with two LEDs at a horizontal distance of 7 cm towards either side of the central fixation point. Subjects were positioned in a distance of 1 m with their eyes at level with the central fixation point. Each finger tapping cycle had a length of 1 s. Simple reaction of the right or left index finger (brief index finger tap) was cued when the right or left LED was switched on, respectively. Within any given cycle, either one of the two LEDs was switched on once for 20 ms (ON for 20 ms, OFF for 980 ms) and timing of the left LED always preceded or was simultaneous to the timing of the right LED. The cued inter-hand phase varied between 0 (in-phase, simultaneous tapping required) and 0.9 in steps of 0.1 (i.e., 10 inter-hand phase conditions). Each of the 10 phases was tested in a separate block of 24 trials, and the blocks were presented in randomized order, separated by 1 min. Reaction time of either index finger was measured from the onset of the go-signal to the onset of the large artifact in the accelerometer signal when the index finger, starting from extension, tapped the resting plate at the end of the flexion movement. We used the onset of this artifact rather than the onset of flexion movement because it was less ambiguous while the latter was often difficult to determine, as index finger extension was often contaminated by physiologic tremor. The onset of the deceleration artifact was determined automatically by an amplitude threshold criterion and confirmed for every single trial by manual cursor setting, using in-house written software (MatLab Version 6.1.0., The Math-Works, Inc., Natick, MA, USA). Vc-BTC performance was defined by calculating observed minus required phase. The difference of the measured inter-hand phase from the cued inter-hand phase was taken as performance deviation.

It is important to note that although the left LED always preceded the right LED (except for in-phase

conditions), the perceived order along the sequence of 24 concatenated tapping cycles typically was the right LED preceding the left LED whenever the physical phase of the right LED in the previous trial to the left LED in the next trial was < 0.5 (i.e., whenever the phase between left and right LED in a given tapping cycle was >0.5, cf. Fig. 1). Therefore, in accordance with the original experiments (Tuller and Kelso 1989), we classified cued phases of 0.1–0.4 as "left-hand leading right-hand conditions" and phases of 0.6-0.9 as "right-hand leading left-hand conditions".

Unimanual motor performance

Subjects were asked to perform 10 s runs of index finger tapping at maximum repetition speed with either their left or right index finger, and the number of taps per run was taken as performance. In addition, they performed the Nine-Hole Peg Test (9-HPT), a highly standardized test for unimanual hand function (Mathiowetz et al. 1985). The 9-HPT was repeated twice for either hand. The time necessary to complete the test was taken as performance, and conditional averages were calculated for either hand.
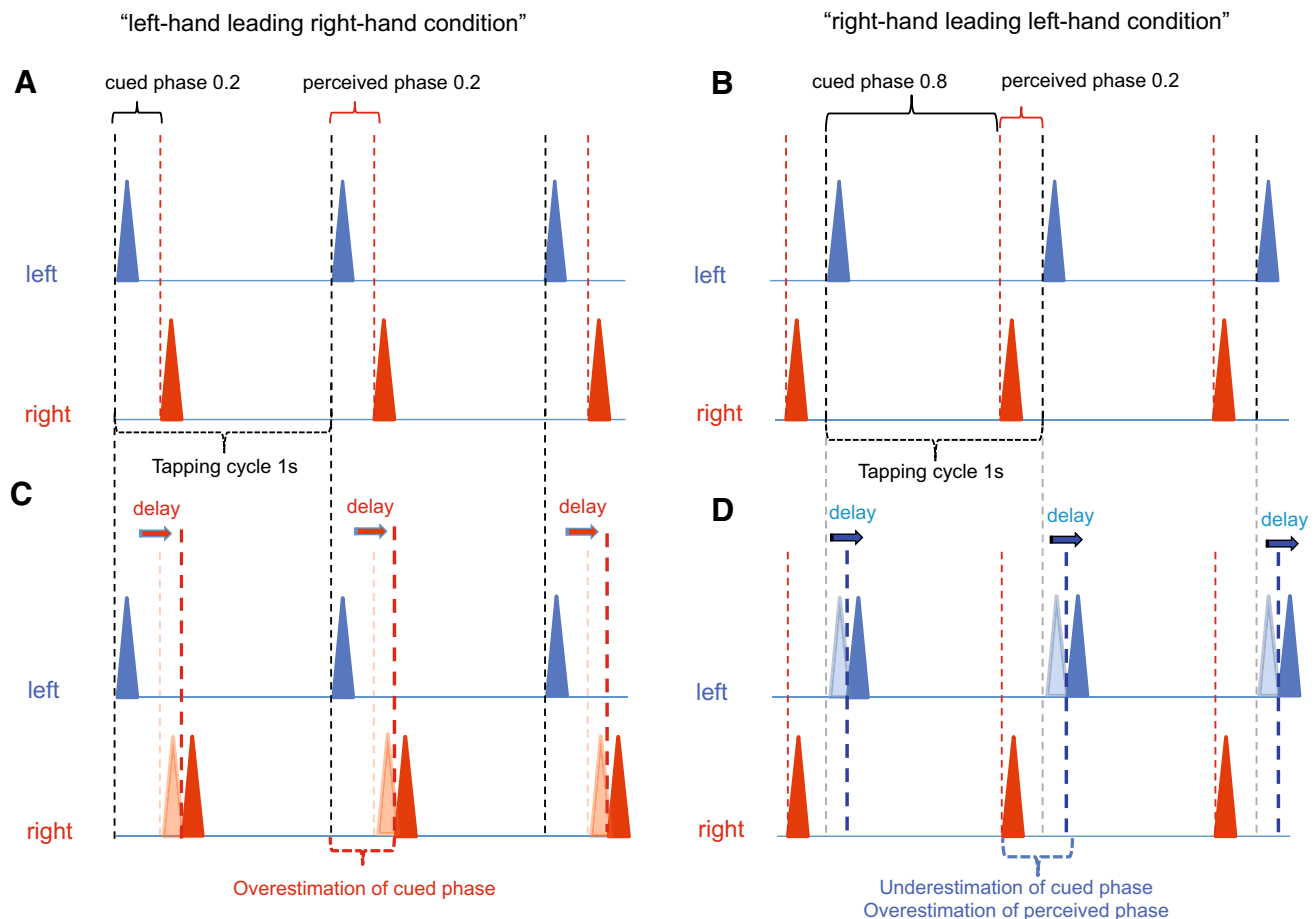
Fig. 1 Schematic design of the visually cued bimanual temporal coordination (vc-BTC) test. The *blue triangles* represent tapping accelerometer artifacts generated when the left index finger hits the resting plate, the *red triangles* represent tapping accelerometer artifacts of the right index finger. Within a given tapping cycle of 1 s duration, the signal of the left LED (cuing index finger tapping of the left hand) always preceded or was simultaneous to the signal of the right LED (cuing index finger tapping of the right hand). The cued inter-hand interval ranged from 0 ms (in-phase, simultaneous tapping required) to 0.9 s in steps of 0.1 s (i.e. 10 inter-hand interval conditions). Reaction time of either index finger was measured from the onset of the LED go-signal to the onset of the tapping artifact. Note, that the perceived interval along the sequence of 24 concatenated tapping cycles typically was left LED leading right LED whenever the cued inter-hand interval within a given tapping cycle

was <0.5 s (**a**), but reversed to right LED leading left LED whenever the interval of the right LED in the previous trial to the left LED in the next trial was <0.5 s (i.e. whenever the interval between left and right LED in a given tapping cycle was >0.5 s) (**b**). *Red triangles* in **c** show a typical example of delayed right index finger tapping produced by healthy subjects with short inter-hand phases (<0.5), i.e., overestimation of the cued delay away from the in-phase attractor. The *light red triangles* in the background indicate the cued right index finger timings. *Blue triangles* in **d** show a typical example of left index finger tapping produced by a healthy subject with long inter-hand phases (>0.5). The finger tapping overestimates the perceived inter-hand interval ("right hand leading left hand"), but underestimates the cued phase, away from the in-phase attractor. *Light blue triangles* in the background indicate the cued left index finger timings

Statistics

Group differences of FA were assessed by an ANOVA with GROUP (healthy controls, CIS, RRMS) as the between-subject effect. Group differences of S-IHI were determined by mixed repeated-measures ANOVA (rmA-NOVA) with GROUP (healthy controls, CIS, RRMS) as between-subject effect and CS INTENSITY (six levels, 100–150 % RMT in 10 % steps) as within-subject effect. Group differences of vc-BTC were assessed by a mixed rmANOVA with GROUP (healthy controls, CIS, RRMS) as the between-subject effect and CUED INTER-HAND PHASE (10 levels, 0–0.9 in steps of 0.1) as within-subject effects. Mauchly's test was used to test for violation of sphericity and the Huynh–Feldt correction applied whenever necessary. Post hoc testing was performed in case of significant main effects or their interaction by using Fisher's PLSD test. In addition, group comparisons were conducted for cued inter-hand phases grouped into small phases (0.1–0.4) and long phases (0.6–0.9) because it had been demonstrated previously that healthy subjects overestimate small intervals but underestimate long intervals (Tuller and Kelso 1989).

The relations of CMF microstructure (FA) to effective connectivity (S-IHI) and vc-BTC performance were analyzed by calculating Pearson correlation coefficients. Furthermore, the influence of S-IHI on the correlation between FA-CC and vc-BTC performance was tested by stepwise multiple linear regression analysis.

For all tests, IBM® SPSS® Statistics (version 22) was used. Statistical significance was assumed if $p < 0.05$. Data are given as mean ± SEM.

Results

Unimanual motor performance

The number of taps at maximum rate over 10 s was not different between GROUPS for the right index finger (healthy controls 57.3 ± 1.8, CIS 54.8 ± 5.1, RRMS 55.6 ± 2.5, $F_2 = 0.24$, $p = 0.79$), or the left index finger (healthy controls 54.2 ± 2.5, CIS 50.5 ± 3.5, RRMS 50.9 ± 2.3, $F_2 = 0.61$, $p = 0.56$).

There was also no effect of GROUP for 9-HPT performances with the right (healthy controls 18.0 ± 0.4 s, CIS 19.9 ± 1.6 s, RRMS 19.0 ± 1.6 s, $F_2 = 1.30$, $p = 0.28$) or left hand (healthy controls 18.1 ± 0.6 s, CIS 20.0 ± 1.4 s, RRMS 19.8 ± 0.7 s, $F_2 = 1.74$, $p = 0.19$).

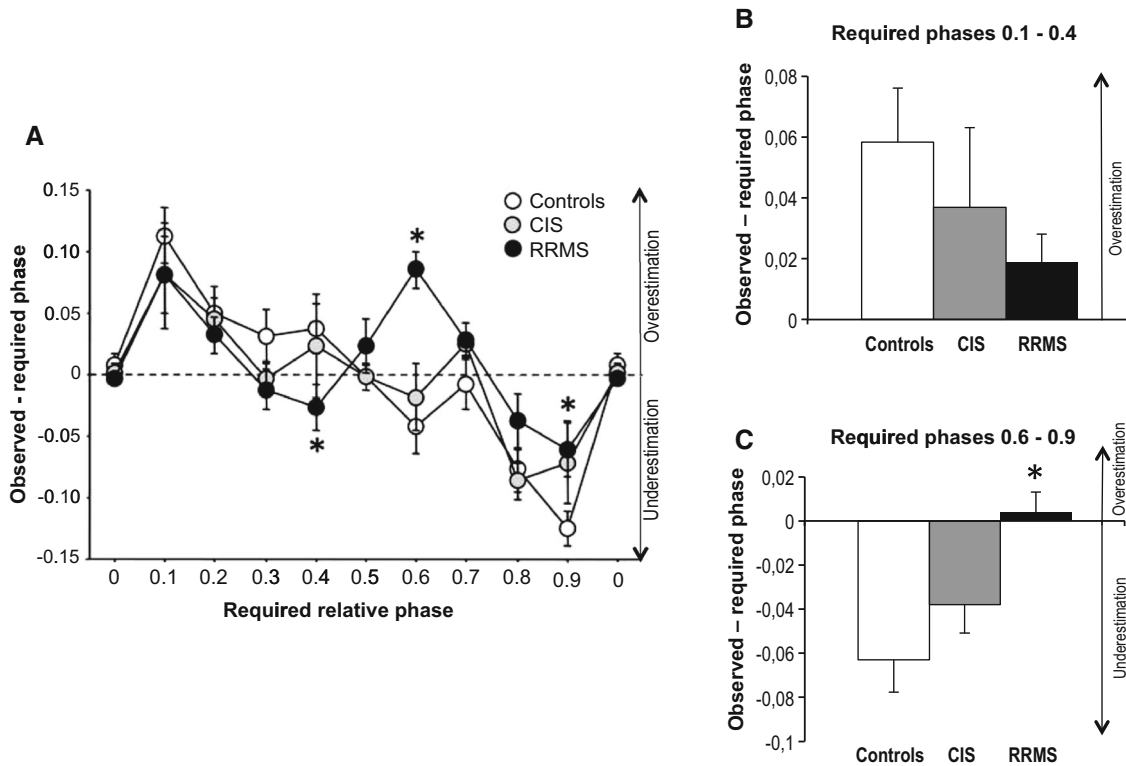## Visually cued bimanual temporal coordination (vc-BTC) performance

In the group of healthy controls, one-sample t tests showed significant performance deviations for the inter-hand phases close to the in-phase condition (phase 0.1, 97.1 ± 16.4 ms, $p < 0.0001$; 0.2, 44.3 ± 11.9 ms, $p = 0.0011$; 0.8, -67.5 ± 11.9 ms, $p < 0.0001$; 0.9, -94.8 ± 12.6 ms, $p < 0.0001$). Hence, the short phases were overestimated, while the long ones were underestimated (Fig. 2a). Therefore, in healthy controls, vc-BTC performance showed deviation *away* from the default in-phase attractor, confirming previous results (Tuller and Kelso 1989).

The mixed rmANOVA for vc-BTC performance did not reveal an effect of GROUP ($F_2 = 1.22$, $p = 0.32$), while the effects of CUED INTER-HAND PHASE ($F_{3.52} = 14.87$, $p < 0.001$) and the interaction of CUED INTER-HAND PHASE with GROUP ($F_{7.03,73.82} = 2.27$, $p = 0.038$) were significant. The significant interaction was explained by the RRMS patients who, when compared to the healthy controls, showed significantly less overestimation at the phase of 0.4, and less underestimation at the phases of 0.6 and 0.9 (Fig. 2a; Table 1). This means that, in accord with the hypothesis, the RRMS patients showed less deviation from the default in-phase attractor. In contrast, CIS patients did not perform differently from healthy controls (Fig. 2a; Table 1).

The mixed rmANOVA of vc-BTC for the short inter-hand phases of 0.1–0.4 (where less overestimation of patients compared to controls or even underestimation means attraction to in-phase movements) did not reveal a significant effect of GROUP ($F_2 = 1.26$, $p = 0.30$) (Fig. 2b). The same analysis for the long inter-hand phases of 0.6–0.9 (where less underestimation or even overestimation means attraction to in-phase movements) showed a significant effect of GROUP ($F_2 = 4.77$, $p = 0.020$). The post hoc comparisons explained this effect by a significant difference between RRMS and healthy controls ($p = 0.006$), with the RRMS patients slightly overestimating the cued inter-hand phases, therefore showing attraction to in-phase movements (Fig. 2c).

Macroscopic hCMF lesions

Conventional T1-weighted and T2-weighted MRI identified hCMF lesions in two patients. The remaining 20 patients were free of macroscopic lesions in the entire hCMF pathway.

Fig. 2 Visually cued bimanual temporal coordination (vc-BTC) performance. **a** Vc-BTC performance is given as observed minus required phase on the y-axis and plotted against the visually cued phase on the x-axis. Positive values indicate overestimation of cued phase, while negative values indicate underestimation. The cued phase of 0 (in-phase movements) is plotted twice with the same data to facilitate comparison with adjacent intervals. *White circles* healthy controls, *gray circles* CIS, *black circles* RRMS. *Asterisks* indicate differences between RRMS and healthy controls (*p* < 0.05). Note that healthy controls overestimated small inter-hand phases (0.1–0.4) but underestimated large inter-hand phases (0.6–0.9), while RRMS patients did so to a lesser extent. This means that deviation away

from in-phase movements was less pronounced in patients with RRMS. This can also be interpreted as stronger attraction to in-phase movements relative to healthy controls. **b** Vc-BTC performance indexed by observed minus required phase pooled for the small inter-hand phases of 0.1–0.4 for the groups of healthy controls (*white bar*), CIS (*gray bar*) and RRMS (*black bar*). There were no significant differences between groups. **c** Observed minus required phase pooled for the large inter-hand phases of 0.6–0.9. RRMS showed a significant difference from healthy controls (**p* < 0.05) by slightly overestimating the cued inter-hand phase and therefore showing attraction to in-phase movements. CIS patients were not different from healthy controls. All data are means ± 1 SEM

Table 1 Inter-hand phase-specific deviations from required phase for the three groups (healthy controls, CIS, RRMS)

Phase	Controls	CIS	RRMS	*p*
0	0.009 ± 0.009	0.002 ± 0.008	−0.003 ± 0.005	0.282
0.1	0.113 ± 0.022	0.081 ± 0.042	0.081 ± 0.031	0.422
0.2	0.051 ± 0.021	0.046 ± 0.018	0.033 ± 0.015	0.501
0.3	0.032 ± 0.021	−0.003 ± 0.012	−0.012 ± 0.017	0.124
0.4	**0.038 ± 0.020**	0.024 ± 0.042	**−0.027 ± 0.018**	0.031
0.5	−0.002 ± 0.011	−0.002 ± 0.010	0.024 ± 0.021	0.310
0.6	**−0.043 ± 0.020**	−0.018 ± 0.027	**0.085 ± 0.015**	<0.001
0.7	−0.008 ± 0.021	0.025 ± 0.009	0.027 ± 0.015	0.195
0.8	−0.077 ± 0.018	−0.086 ± 0.014	−0.038 ± 0.023	0.208
0.9	**−0.124 ± 0.014**	−0.072 ± 0.033	**−0.060 ± 0.022**	0.034

Bold face indicates significant differences between the RRMS and control group. Differences between CIS and control group were not significant for any of the inter-hand phases. The data are also represented in Fig. 2A
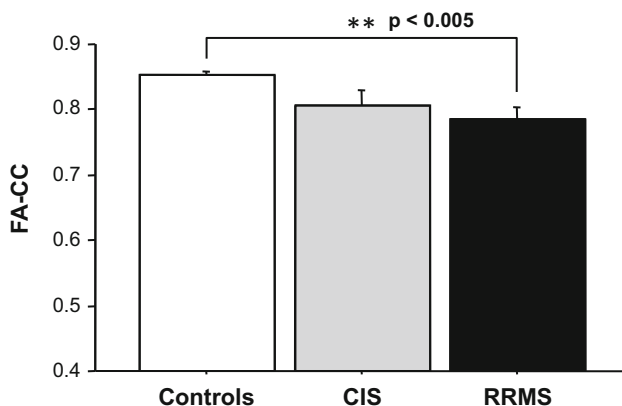
Fractional anisotropy of hand callosal motor fibers (FA-hCMF)

The ANOVA of FA-CC revealed a significant effect of GROUP ($F_2 = 4.80$, $p = 0.015$). Post hoc testing showed that this effect was explained by a significantly lower FA-hCMF in the RRMS patients compared to the healthy controls (0.787 ± 0.017 vs. 0.852 ± 0.007; $p = 0.002$, Fig. 3), while the differences between CIS (0.805 ± 0.026) and healthy controls ($p = 0.12$) and between CIS and RRMS ($p = 0.56$) were not significant (Fig. 3).
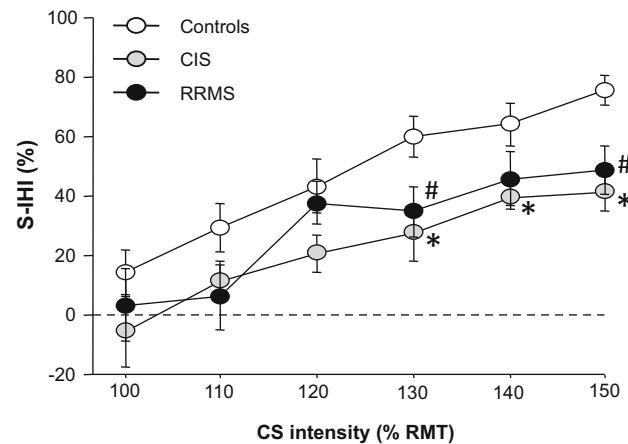
Short interval interhemispheric inhibition (S-IHI)

Resting motor thresholds (RMT, given in % of maximum stimulator output) evoked over the left $M1_{HAND}$ did not differ between groups (healthy controls 42.9 ± 8.7 %, CIS 37.4 ± 6.4 %, RRMS 37.7 ± 6.2 %). Likewise, MEP amplitudes elicited by the CS in the intensity range from 130 to 150 % RMT applied to the left $M1_{HAND}$ did not reveal significant effects for GROUP ($F_2 = 2.52$, $p = 0.10$), or the interaction between GROUP and CS INTENSITY ($F_{2,30} = 1.34$, $p = 0.28$). Finally, there were no significant differences of the mean test MEP amplitudes evoked over the right $M1_{HAND}$ of healthy controls, CIS and RRMS patients (healthy controls 1.02 ± 0.09 mV, RRMS 1.1 ± 0.12 mV, CIS 0.98 ± 0.07 mV). This nil findings are important because they indicate that differences in the stimulation parameters cannot account for the group differences in S-IHI.

ANOVA of S-IHI revealed a significant effect of GROUP ($F_2 = 3.45$, $p = 0.044$; Fig. 4) and CS INTENSITY ($F_{3.02} = 23.70$, $p < 0.001$) while the interaction of GROUP with CS INTENSITY was not significant ($F_{6.04,93.64} = 0.62$, $p = 0.71$). Post hoc testing using
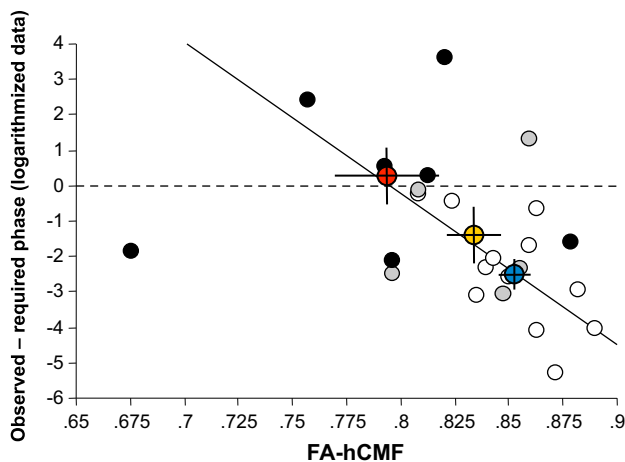

Fig. 4 Short interval interhemispheric inhibition (S-IHI) intensity curves. S-IHI (y-axis) was tested from the left $M1_{HAND}$ to the right $M1_{HAND}$ and is given as ($1 -$ conditioned MEP/unconditioned MEP) $\times$ 100 % (i.e., larger values indicate stronger S-IHI) and plotted against intensity of the conditioning stimulus (x-axis, in % of the RMT). All data (*white circles* healthy controls, *gray circles* CIS, *black circles* RRMS) are group means $\pm$ 1 SEM. Note that both, CIS and RRMS showed significantly reduced S-IHI (pooled across all CS intensities) compared to healthy controls ($p = 0.025$ and $p = 0.044$, respectively). *Asterisks* and *hashes* indicate significant differences at specific CS intensities between CIS and healthy controls, and between RRMS and healthy controls, respectively ($p < 0.05$)

Fisher's PLSD revealed reduced S-IHI (across all CS intensities) in the RRMS patients compared to healthy controls ($p = 0.044$), and in CIS patients compared to the healthy controls ($p = 0.025$), whereas RRMS and CIS patients were not different from each other ($p = 0.51$; Fig. 4).

Correlation between FA-hCMF and vc-BTC performance

For the healthy controls, correlation analysis between FA-hCMF and "right-hand leading left-hand" vc-BTC performance (data pooled for cued inter-hand phases of 0.6–0.9, logarithmically transformed) revealed a significant inverse linear correlation ($r = -0.65$, $p = 0.021$), indicating that higher FA values were associated with a stronger deviation (underestimation of the cued inter-hand interval) from in-phase movements (regression line in Fig. 5). In the healthy subjects, linear regression analysis between FA-hCMF and "left-hand leading right-hand" vc-BTC performance (data pooled for cued inter-hand phases of 0.1–0.4, logarithmically transformed) did not reveal a significant correlation ($p = 0.28$, data not shown). Detailed data of two representative healthy controls with above vs. below average values, respectively, for S-IHI, FA-hCMF and vc-BTC performance as indicated by deviation from the cued inter-hand phase are given in Fig. 7a, b.

Fig. 3 Fractional anisotropy of hand callosal motor fibers (FA-hCMF). FA-hCMF was significantly reduced in RRMS (*black bar*) compared to healthy controls (*white bar*, **$p < 0.005$), whereas CIS (*gray bar*) did not differ from healthy controls or RRMS. All data are mean $\pm$ SEM

Fig. 5 Correlation between FA-hCMF and vc-BTC performance. The correlation of FA-hCMF (*x*-axis) with vc-BTC performance given as observed minus required phase (data pooled for the large phases of 0.6–0.9, negative values mean an underestimating deviation from the in-phase attractor, data logarithmically transformed) revealed a significant linear inverse correlation in healthy controls (*white circles*, $r = -0.65$, $p = 0.021$, regression line indicated). This correlation was absent in CIS (*gray circles*, $p = 0.79$) and RRMS (*black circles*, $p = 0.80$). Coordinates of group means $\pm$ 1 SEM are indicated by *colored circles* (*blue* healthy controls, *yellow* CIS, *red* RRMS). Note that the group means of patients are shifted along the regression line of the healthy controls towards less FA-hCMF and less deviation from the attractor of in-phase movements

While the pooling across short (phases from 0.1 to 0.4) and long (phases from 0.6 to 0.9) inter-hand phases was justified by the previous results of Tuller and Kelso (1989) we additionally ran the correlation analyses in the group of healthy controls also for the individual phases. We found that vc-BTC at some but not all of the phases correlated significantly with FA-hCMF. Significant correlations or trends were found with the phases of 0.4 ($r = 0.658$, $p = 0.020$), 0.6 ($r = -0.556$, $p = 0.061$) and 0.7 ($r = -0.547$, $p = 0.066$).

The CIS and RRMS groups did not show significant linear correlations between FA-hCMF and vc-BTC (CIS: $p = 0.79$, RRMS: $p = 0.80$; Fig. 5). Also there was no significant correlation when data from CIS and RRMS patients were pooled ($p = 0.89$). The coordinates of the group averages of FA-hCMF (*x*-axis) and vc-BTC performance (*y*-axis) were located on the regression line of the healthy controls, but shifted (RRMS more than CIS) towards lower FA-hCMF and less deviation from in-phase movements (colored circles in Fig. 5).

Correlation between S-IHI and vc-BTC performance

In the healthy controls, analysis of the relation between S-IHI and vc-BTC performance, i.e., deviation from cued inter-hand interval for the long intervals (data pooled for

cued inter-hand phases of 0.6–0.9, logarithmically transformed) revealed a significant inverse linear correlation ($r = -0.61$, $p = 0.03$) (Fig. 6), indicating that subjects with stronger S-IHI from the left $M1_{HAND}$ to the right $M1_{HAND}$ show stronger deviation (more negative values) from in-phase movements. Data from two representative healthy controls are shown in Fig. 7a, b. No correlation was found between S-IHI and vc-BTC performance at short phases (pooled data for 0.1–0.4) ($p = 0.29$). This indicates functional specificity of S-IHI from the left $M1_{HAND}$ to the right $M1_{HAND}$ for those BTC conditions (long phases) when tapping of the right hand (guided by activity in the left $M1_{HAND}$) in a given trial leads tapping of the left hand (guided by activity in the right $M1_{HAND}$) in the next trial. CIS and RRMS did not show significant correlations between S-IHI and vc-BTC performance, neither for short nor long phases (all $p > 0.05$). Also, no correlations between S-IHI and vc-BTC performance were found when data from CIS and RRMS patients were pooled (all $p > 0.05$). The coordinates of the group averages of S-IHI (*x*-axis) and vc-BTC performance (pooled data of phases of 0.6–0.9, logarithmically transformed, *y*-axis) deviated from the regression line of the healthy controls, with RRMS patients shifted disproportionately towards in-phase movements (colored circles in Fig. 6).
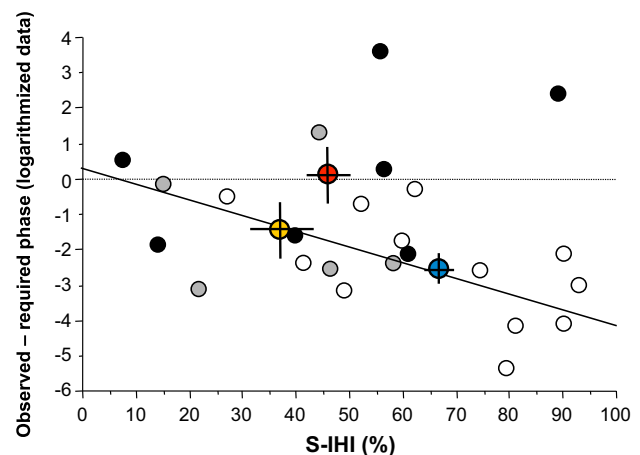
Fig. 6 Correlation between S-IHI and vc-BTC performance. The correlation between S-IHI (*x*-axis, given as ($1 -$ conditioned MEP/ unconditioned MEP) $\times$ 100 %, i.e., larger values indicate stronger S-IHI) and the vc-BTC performance given as observed minus required phase for the "right-hand leading left-hand condition" (data pooled for the large phases of 0.6–0.9, negative values mean an underestimating deviation from the in-phase attractor, logarithmically transformed) revealed a significant inverse correlation in healthy controls (*white circles*, $r = -0.61$, $p = 0.03$). This correlation means that subjects with stronger S-IHI from the left $M1_{HAND}$ to the right $M1_{HAND}$ showed stronger deviation (more negative values) from in-phase movements. Note that this correlation was absent in CIS (*gray circles*) and RRMS (*black circles*). Coordinates of group means $\pm$ 1 SEM are indicated by *colored circles* (*blue* healthy controls, *yellow* CIS, *red* RRMS)
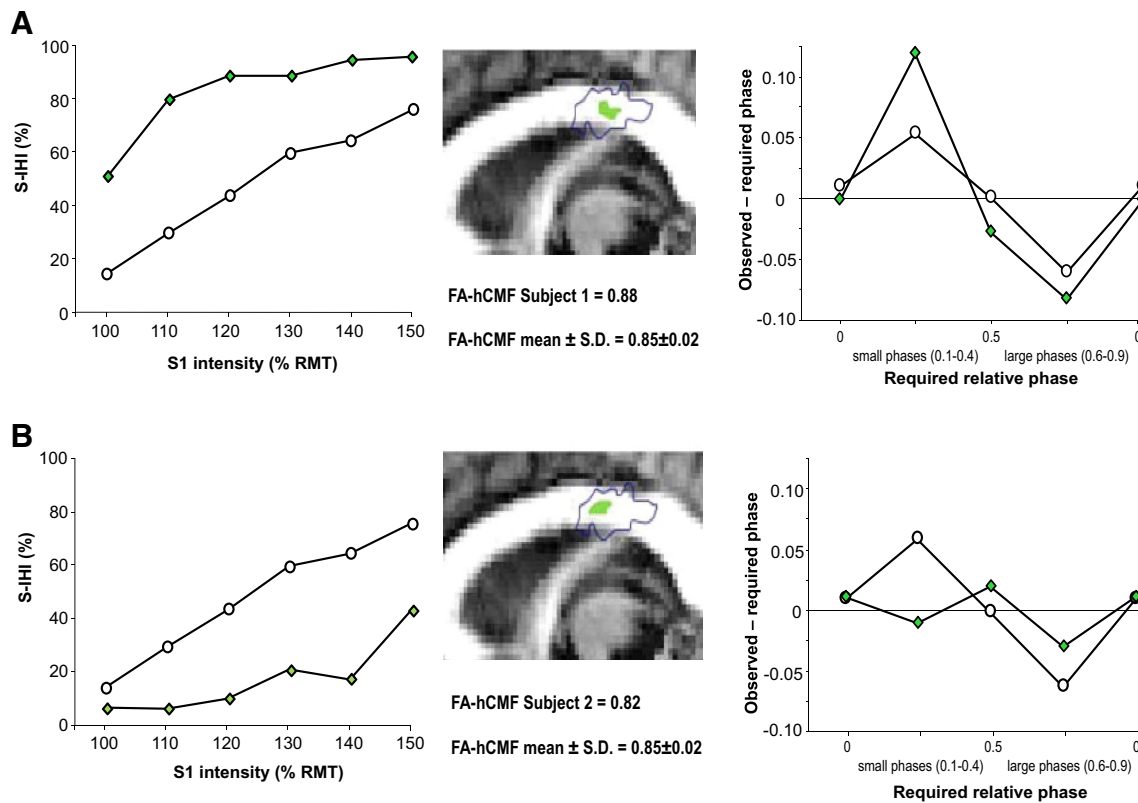
Fig. 7 Link between effective connectivity (S-IHI), anatomical connectivity (FA-hCMF) and visually cued bimanual temporal coordination (vc-BTC) performance in two representative healthy controls. *Left panels* S-IHI of each index subject (*green diamonds*) is given as (1 − conditioned MEP/unconditioned MEP) × 100 % (*y*-axis) and plotted against CS intensities (in % RMT, *x*-axis) in relation to the mean S-IHI intensity curve of all healthy controls (*white circles*). *Middle panels* FA-hCMF derived from each subject's individual tractography data (*green areas*). *Purple* contours are the outline of tractography data from all healthy controls. The corresponding FA-hCMF for the index subject and the mean FA-hCMF ± SD from all healthy controls are indicated. *Right panels* vc-BTC performance is given as observed minus required phase on the *y*-axis and plotted against required phase on the x-axis for each index subject (*green diamonds*) in relation to the mean vc-BTC performance of all healthy controls (*white circles*). Data points for cued small phases (0.1–0.4) and large phases (0.6–0.9) are grouped. Note that the index subjects in **a** vs. **b** exhibited above vs. below average values, respectively, for S-IHI, FA-hCMF and deviation from required phase in the out-of-phase vc-BTC conditions

Stepwise multiple linear regression analysis

The Pearson correlation matrix reflecting the bivariate linear regression analyses in the group of healthy controls showed significant correlations for all pairs of variables: S-IHI vs. vc-BTC: $r = -0.577$, $p = 0.049$; FA-hCMF vs. vc-BTC: $r = -0.651$, $p = 0.022$; S-IHI vs. FA-hCMF: $r = 0.640$, $p = 0.025$. The stepwise multiple regression analysis revealed that FA-hCMF significantly predicted vc-BTC ($r = -0.651$, $p = 0.022$) but that the addition of S-IHI did not improve the correlation ($r = 0.683$, $p = 0.059$). The partial correlation of S-IHI with vc-BTC (i.e., after partialing out FA-hCMF) was only $r = -0.276$, $p = 0.412$. This means that, although S-IHI correlated with vc-BTC and FA-hCMF, it did not significantly contribute to the correlation between FA-hCMF and vc-BTC.

Discussion

In line with our hypothesis, we provided first time evidence that in healthy subjects, anatomical and effective connectivity of the hand areas of the primary motor cortices in the right and left hemisphere through hand callosal motor fibers (hCMF) predict visually cued bimanual temporal coordination (vc-BTC) performance. We further demonstrated that these associations are significantly altered in patients with CIS and early-stage RRMS. These findings will be discussed in detail in the following paragraphs.

Visually cued bimanual temporal coordination (vc-BTC) performance

A large body of work showed that certain bimanual coordination patterns can be performed with less effort and

greater stability than others (Yamanishi et al. 1980; Tuller and Kelso 1989; Swinnen 2002; Johansen-Berg et al. 2007; Kovacs and Shea 2011). Asynchronous irregular phasing is fragile and susceptible to in-phase and anti-phase attraction. But even with respect to these two most stable movement patterns, in-phase and anti-phase, stability variation have been found. As movement cycle frequency increases, anti-phase movements collapse into in-phase movements, in a way that the non-dominant hand joins into the cycle of the dominant hand (Byblow et al. 1994; Jirsa et al. 1998; Kelso et al. 1981; Kelso 1984). The degrees as to which default synchronous oscillators influence a given BTC task highly depends on the mode of cueing. Self-paced performance of out-of-phase finger tapping from memory has been demonstrated most vulnerable to influences of in-phase oscillators, such that in the vicinity of the in-phase and anti-phase conditions, the performer is pulled towards these attractors (Yamanishi et al. 1980). In contrast, visually cued BTC (vc-BTC) is characterized by the opposite tendency, as in the vicinity of in-phase conditions, most of the performers overestimate the cued interval (Tuller and Kelso 1989). As an example, in the vc-BTC task of Tuller and Kelso, an average relative phase of about 0.16 was performed when a phase of 0.1 was externally cued. In accord with the data of Tuller and Kelso (1989), we found that healthy subjects systematically overestimated short (0.1–0.4) and underestimated long cued inter-hand phases (0.6–0.9), resulting in a deviation away from in-phase movements. The aim of the present study was to reveal the neuroanatomical and functional correlates that drive vc-BTC performance away from in-phase movements.

Before the invention of modern structural and functional imaging, the role of the CC in bimanual coordination mainly had been studied in various pathological conditions. Patients with structural CC damage exhibited degradation of spatial and temporal components of bimanual coordination, pointing to the crucial importance of transcallosal information transfer (Caille et al. 2005; Kennerley et al. 2002; Preilowski 1972; Serrien et al. 2001; Tuller and Kelso 1989; Caeyenberghs et al. 2011; Bonzano et al. 2014; Wittstock et al. 2010). After a first-step partial section of the anterior CC in a patient with intractable epilepsy, deterioration of bimanual movement synchronization specifically for self-initiated movements was observed. However, a drastic performance decline for visually cued bimanual movements became evident after a second-step section of the posterior CC (Eliassen et al. 2000). This suggested that the posterior CC, where the CMFs are located (Zarei et al. 2006; Wahl et al. 2007; Hofer and Frahm 2006; Fling et al. 2013), is involved in vc-BTC. Because we wanted to investigate behavior generated by hCMFs, we deliberately chose a protocol that tests visually cued rather than self-paced BTC in an index

finger tapping task (Tuller and Kelso 1989) and confirmed, that in healthy subjects, FA-hCMF predicts vc-BTC performance (Fig. 5).

Imaging techniques sensitive enough to detect the relatively subtle interindividual white matter microstructural differences in healthy individuals have only emerged in the last decade. Since then, several studies have examined the relationship between bimanual task performance and callosal microstructure in healthy individuals (Muetzel et al. 2008; Johansen-Berg et al. 2007; Sullivan et al. 2001; Serbruyns et al. 2013; Fling et al. 2011; Gooijers et al. 2013). For example, Sullivan et al. (2001) reported correlations between FA in the splenium of the CC and alternating finger tapping performance in a cross-sectional analysis of healthy adults (Sullivan et al. 2001). In a large group of 9- to 23-year-old subjects, anti-phase bimanual finger tapping performance improved with the maturation of the CC as assessed by FA (Muetzel et al. 2008). However, since no tractography was employed, those studies did not allow unequivocal anatomical attribution of the investigated behaviors to defined interhemispheric pathways.

While the earlier correlation studies used a simple paradigm by testing anti-phase tapping speed, recent studies employed more complex bimanual task conditions, requiring varying degrees of interhemispheric interaction. Gooijers et al. (2013) showed that the positive correlation between FA values in the motor and the occipital region of the CC and the performance in tracking a target on a screen by rotating two dials with both hands according to five inter-hand frequency ratios (1:1, 3:1, 3:2, 2:3, 1:3) was especially pronounced in the presence of visual task enhancement (Gooijers et al. 2013). Learning success of the more complex nonpreferred interhand frequency ratios of this task (3:2, 2:3) was predicted by higher FA values of the genu of the CC, which contains dense interhemispheric projections between the prefrontal cortices (Sisti et al. 2012). Interesting examples on how microstructural variation in CC subregions relates to bimanual performance have also been provided by recent work on elderly participants. FA values in the subregions of the CC connecting occipital, primary motor, sensory and premotor cortices were positively correlated with performance on a bilateral precision/object manipulation task, simultaneous finger tapping speed, a complex bimanual rotation task and movement speed in a bimanual choice reaction time test. Such associations were less prominent in a younger group (Serbruyns et al. 2013).

Our findings regarding the association of callosal topography and behavior are in closest accord with those of one previous study (Johansen-Berg et al. 2007), which also identified the posterior midbody of the CC as the site of correlation between FA and bimanual coordination performance. However, they diverge significantly in their

appraisal of the specific role of CMFs. In the former study, probabilistic tractography showed rich connections of the CC with medial wall areas, but a striking absence of fibers interconnecting $M1_{HAND}$. This would implicate that inter-hemispheric connections between medial wall areas such as the supplementary motor area and the caudal cingulate motor area, rather than the hCMFs are critical for bimanual coordination. Although this is compatible with anatomical findings in macaque monkeys that showed scarcity of hCMFs (Rouiller et al. 1994), the present study contradicts this view as it suggests that hCMFs play a pivotal role in BTC abilities of humans. Different methodological approaches employed in the two studies likely account for the divergent findings: Johansen-Berg et al. (2007) used clusters resulting from previous global FA statistics of the CC as ROIs for consecutive tractography. In contrast, selective examination of hand CMFs was performed in the present study, and only then quantitative structural and functional information strictly confined to this fiber system was extracted. Furthermore, Johansen-Berg et al. (2007) used a completely different behavioral approach, by investigating the differential stability of the two intrinsic phasing patterns (in-phase and anti-phase) in relation with integrity measures of the CC. In line with previous work (Kelso et al. 1981; Kelso 1984; Stephan et al. 1999; Byblow et al. 1994) they showed, that when cycle frequency is scaled, the anti-phase pattern is vulnerable to interference by the in-phase pattern at a critical frequency, indicating superior stability of the latter. Lower FA in the CC was associated with de-stabilization of the anti-phase pattern at lower frequencies. However, none of the studies discussed above provided a neurophysiological mechanism to explain the behavior of interest by employing a measure of functional or effective connectivity.

In the present experiments, we assumed that especially those vc-BTC patterns intermediate between in-phase and anti-phase depend on the integrity of hCMFs. Unlike all previous work, we strictly focused our investigation on the role of the CMFs interconnecting the $M1_{HAND}$ of the two hemispheres. We showed here, to the best of our knowledge for the first time, that in healthy subjects, hCMF effective connectivity as measured by S-IHI predicts vc-BTC performance (cf. Fig. 6): strong S-IHI was associated with stronger deviation away from in-phase movements. This finding is in accord with previous work from our group where we showed an inverse correlation between S-IHI and EMG mirror activity, i.e., unwanted co-activation during intended unimanual contraction of the homonymous muscle of the other side (Hübers et al. 2008). This EMG mirror activity can be conceived as an index of "in-phase" activation of homonymous M1 motor representations. This default mode activation pattern in the distributed bi-hemispherical motor network (for review,

Swinnen 2002; Gooijers and Swinnen 2014), needs to be actively suppressed when out-of-phase bimanual movements are required. The present data strongly suggest that microstructural integrity (FA-hCMF) and effective connectivity (S-IHI) of the hand CMFs significantly contribute to the suppression of unwanted bilateral in-phase activation of $M1_{HAND}$.

Using vc-BTC we confirmed previous data (Tuller and Kelso 1989) that healthy subjects are driven away from in-phase movements when they are required to perform out-of-phase movements in the vicinity of the in-phase condition. Nevertheless, we hold on to the concept of in-phase attraction, as did Tuller and Kelso. The observed vc-BTC patterns represent the net effect behavior resulting from the influence of coupled in-phase oscillators (in the two hemispheres) on the one hand, and deviation away from in-phase movements put into effect through acquired interhemispheric inhibition (IHI) on the other hand.

To what extent in-phase attraction, or deviation away from in-phase conditions are predominantly expressed, most likely depends on the task characteristics, the degree of experience, developmental maturation of the motor CC, and the structural and functional integrity of the motor CC. Vollmann et al. (2014) showed, that the relationship between S-IHI and FA in the CC can be modified by different musical training regimes (Vollmann et al. 2014). They compared piano players, string players and non-musicians and showed that S-IHI was generally stronger in musicians, but differed significantly from non-musicians only in string players. S-IHI in string players correlated with FA in the posterior midbody, while S-IHI in pianists was comparable to that of non-musicians and did not show significant structure–function relationship in the CC. This indicated instrument specific use-dependent plasticity in both functional (S-IHI) and structural (FA) connectivity under high demands of asynchronous asymmetric bimanual temporal coordination (Vollmann et al. 2014). This is in accord with our finding that those subjects with the highest FA-hCMF and S-IHI showed the largest temporal offsets between hands in the out-of-phase conditions away from the in-phase condition. Finally, as a brief note of caution, we did not use navigated TMS for the S-IHI measurements. Therefore, we have no direct information on the topographical match of the TMS hotspots in $M1_{HAND}$ and the fMRI defined M1HAND representations used for hCMF tractography. Although previous studies reported Euclidean differences between navigated TMS hotspots and fMRI local activation maxima of about 10 mm (Weiss et al. 2013; Ruohonen and Karhu 2010), we do not think that lack of this information is critical in the present study, as we found significant correlations of both S-IHI and FA-hCMF with vc-BTC performance, signifying that both

measures very likely targeted the same transcallosal pathway relevant for visually guided bimanual coordination.

Findings in patients with multiple sclerosis

In skilled subjects, Yamanishi et al. (1979) showed that attraction to stable in-phase decreases with the amount of training. They suggested that the interaction between the two synchronous oscillators is weakened by learning of asynchronous patterns (Yamanishi et al. 1979). While subjects highly trained in the BTC paradigm showed less attraction to synchrony even when self-paced (Yamanishi et al. 1979), patients with callosotomy showed high penetrance of default in-phase oscillation (Tuller and Kelso 1989). This is in line with our data in early-stage RRMS. In the vicinity of in-phase tapping, patients were also driven away from in-phase movements, but to a significantly lesser degree than healthy controls. Reduced S-IHI and FA-hCMF implicate that this might be due to motor callosal disconnection.

Although macroscopic CMF lesions were detectable in two patients only, RRMS patients showed significantly reduced FA-hCMF (Fig. 3). This is consistent with the findings of other studies, that diffusion abnormalities in the CC can be present at the earliest stages of multiple sclerosis (Bonzano et al. 2008; Harrison et al. 2011; Sigal et al. 2012; Wahl et al. 2011), before atrophy or macroscopic lesions are detectable by conventional MRI (Ranjeva et al. 2003; Wahl et al. 2011), and before diffusion abnormalities are detectable in normal appearing white matter (NAWM) elsewhere in the brain (Ge et al. 2004; Harrison et al. 2011). In addition, we found a graded pathology, as the FA-hCMF of the CIS group ranged in between those of the healthy controls and RRMS (Fig. 3). A similar graded FA pathology has been described in two other studies that compared FA in the NAWM of CIS and RRMS patients (Pulizzi et al. 2007; Yu et al. 2008). In contrast, this graded pathology was not detectable for effective connectivity, as both groups showed equally pronounced reductions of S-IHI. This suggests that compared to FA-hCMF, S-IHI constitutes an even more sensitive marker of early disease pathology. In contrast, FA-hCMF might be superior for disease staging and estimation of tissue damage severity.

Compared to healthy subjects that over-emphasize deviation from the in-phase attractor, RRMS patients showed significantly more attraction to in-phase movements. These findings confirm and extend previous reports on bimanual motor coordination abnormalities in more advanced stages of MS (Bonzano et al. 2008; Larson et al. 2002). Also, in agreement with our findings, one recent study demonstrated significant alterations in motor performance even in early RRMS patients with an EDSS of 0

when a weighted combination of unimanual and bimanual coordination measures was used (Bonzano et al. 2013). However, that study also found significant alterations in unimanual performance in patients with early RRMS. In contrast, we found altered BTC performance in the presence of normal motor performance in unimanual motor tasks (finger tapping at maximum rate, 9-HPT). Our findings, therefore, support the notion that integrity of hCMFs is essential for vc-BTC performance and emphasize that the CC is a preponderant site of early disease activity.

CIS and RRMS patients showed a breakdown of the relations between FA-hCMF and S-IHI with vc-BTC (Figs. 5, 6). The reasons for this dissociation can only be speculated upon. Functional MRI studies in multiple sclerosis patients with defined structural brain damage have shown stronger activation of cortical areas, increased connectivity and recruitment of additional cortical areas (Au Duong et al. 2005; Audoin et al. 2005; Rocca et al. 2005, 2007; Staffen et al. 2002; Gamboa et al. 2014; Giorgio et al. 2010) as well as decreased fMRI activity in specific task related areas (Penner et al. 2003; Rocca et al. 2010). Enhancement and redistribution of functional activity and connectivity might serve the purpose of limiting the behavioral manifestations of disease-related injury. Recruitment of a widespread bihemispheric motor network was also found after ischemic damage of the CC and was paralleled by bimanual recoupling in response to visual cues (Seitz et al. 2004). Therefore, it is well possible that the breakdown of a normally tight relation between structure, function and behavior can be explained by network reorganization along pathways other than the hand CMFs to support BTC abilities.

To the best of our knowledge, this is the first study that simultaneously investigated the impact of both, interhemispheric microstructural integrity and effective connectivity along fiber tracts connecting $M1_{HAND}$ on BTC. There is only one previous study that also employed three levels of investigation and found fundamental differences in callosal structure, effective connectivity and bimanual control between young and older adults (Fling and Seidler 2012). That study revealed significantly higher callosal FA values and a trend for a longer duration of the ipsilateral silent period, another putative marker of hCMF effective connectivity (Meyer et al. 1995) in young compared with older adults. Surprisingly, Fling and Seidler (2012) showed that higher FA values in the CC area connecting primary motor cortices and longer ipsilateral silent periods were associated with poorer performance on a bimanual differential force production task. This was in line with one previous study by the same group (Fling et al. 2011) that reported association of higher FA values in the posterior CC with less accuracy in an out-of-phase tapping task in

young adults. Bearing in mind, that in previous studies, higher FA values were associated with better performance on asynchronous movements (Johansen-Berg et al. 2007), these results may seem counterintuitive at first sight. Among the possible explanations for the unexpected results, the authors favored excessive mutual inhibition during out-of-phase bimanual tasks (Fling and Seidler 2012). In essence, this view is in close accord with our present findings, where higher S-IHI und FA-hCMF were associated with stronger intermanual offsets, i.e., over- or underestimation of the required relative phase away from the in-phase attractor.

With respect to accuracy of interval timing, patients with multiple sclerosis showed superior performance as they deviated less from the cued inter-hand interval compared to healthy controls. Therefore, the present study delivers a rare, yet not unique example of superior bimanual coordination performance in the pathological- compared to the healthy condition. For spatial coupling, Franz and colleagues (1996) demonstrated superior skills in callosotomy patients when intermanual uncoupling was required in order to draw conflicting trajectories. The superior performance was explained by the release from interhemispheric interference by conflicting information. Using the same bimanual paradigm, these findings were replicated in patients with partial callosotomy, but only in patients with section of the posterior third of the CC (Eliassen et al. 1999, 2000). However, for temporal coupling, we are not aware of any previous studies that demonstrated superior performance in pathological CC conditions.

Conclusions

Our findings support the notion that anatomical and effective connectivity of callosal motor fibers in healthy subjects are tightly correlated with visually cued out-of-phase bimanual temporal coordination performance. In early-stage multiple sclerosis, callosal connectivity and out-of-phase bimanual temporal coordination performance are already altered to significant extent. This indicates an important role of the motor corpus callosum in bimanual coordination and suggests that multimodal assessment of motor callosal function represents a diagnostic index of early pathology in this disease.

References

Au Duong MV, Boulanouar K, Audoin B, Treseras S, Ibarrola D, Malikova I, Confort-Gouny S, Celsis P, Pelletier J, Cozzone PJ, Ranjeva JP (2005) Modulation of effective connectivity inside the working memory network in patients at the earliest stage of multiple sclerosis. NeuroImage 24(2):533–538

Audoin B, Au Duong MV, Ranjeva JP, Ibarrola D, Malikova I, Confort-Gouny S, Soulier E, Viout P, Ali-Cherif A, Pelletier J, Cozzone PJ (2005) Magnetic resonance study of the influence of tissue damage and cortical reorganization on PASAT performance at the earliest stage of multiple sclerosis. Hum Brain Mapp 24(3):216–228

Basser PJ, Pierpaoli C (1996) Microstructural and physiological features of tissues elucidated by quantitative-diffusion-tensor MRI. J Magn Reson B 111(3):209–219

Bonzano L, Tacchino A, Roccatagliata L, Abbruzzese G, Mancardi GL, Bove M (2008) Callosal contributions to simultaneous bimanual finger movements. J Neurosci 28(12):3227–3233

Bonzano L, Sormani MP, Tacchino A, Abate L, Lapucci C, Mancardi GL, Uccelli A, Bove M (2013) Quantitative assessment of finger motor impairment in multiple sclerosis. PLoS One 8(5):e65225. doi:10.1371/journal.pone.0065225

Bonzano L, Tacchino A, Brichetto G, Roccatagliata L, Dessypris A, Feraco P, Lopes De Carvalho ML, Battaglia MA, Mancardi GL, Bove M (2014) Upper limb motor rehabilitation impacts white matter microstructure in multiple sclerosis. NeuroImage 90:107–116. doi:10.1016/j.neuroimage.2013.12.025

Byblow WD, Carson RG, Goodman D (1994) Expressions of asymmetries and anchoring in bimanual coordination. Hum Mov Sci 13(1):3–28. doi:10.1016/0167-9457(94)90027-2

Caeyenberghs K, Leemans A, Coxon J, Leunissen I, Drijkoningen D, Geurts M, Gooijers J, Michiels K, Sunaert S, Swinnen SP (2011) Bimanual coordination and corpus callosum microstructure in young adults with traumatic brain injury: a diffusion tensor imaging study. J Neurotrauma 28(6):897–913. doi:10.1089/neu.2010.1721

Caille S, Sauerwein HC, Schiavetto A, Villemure JG, Lassonde M (2005) Sensory and motor interhemispheric integration after section of different portions of the anterior corpus callosum in nonepileptic patients. Neurosurgery 57(1):50–59

Eliassen JC, Baynes K, Gazzaniga MS (1999) Direction information coordinated via the posterior third of the corpus callosum during bimanual movements. Exp Brain Res 128(4):573–577

Eliassen JC, Baynes K, Gazzaniga MS (2000) Anterior and posterior callosal contributions to simultaneous bimanual movements of the hands and fingers. Brain 123(Pt 12):2501–2511

Evangelou N, Esiri MM, Smith S, Palace J, Matthews PM (2000a) Quantitative pathological evidence for axonal loss in normal appearing white matter in multiple sclerosis. Ann Neurol 47(3):391–395

Evangelou N, Konz D, Esiri MM, Smith S, Palace J, Matthews PM (2000b) Regional axonal loss in the corpus callosum correlates with cerebral white matter lesion volume and distribution in multiple sclerosis. Brain 123(Pt 9):1845–1849

Ferbert A, Priori A, Rothwell JC, Day BL, Colebatch JG, Marsden CD (1992) Interhemispheric inhibition of the human motor cortex. J Physiol (Lond) 453:525–546

Fling BW, Seidler RD (2012) Fundamental differences in callosal structure, neurophysiologic function, and bimanual control in young and older adults. Cereb Cortex 22(11):2643–2652. doi:10.1093/cercor/bhr349

Fling BW, Walsh CM, Bangert AS, Reuter-Lorenz PA, Welsh RC, Seidler RD (2011) Differential callosal contributions to bimanual

control in young and older adults. J Cogn Neurosci 23(9):2171–2185. doi:10.1162/jocn.2010.21600

Fling BW, Benson BL, Seidler RD (2013) Transcallosal sensorimotor fiber tract structure-function relationships. Hum Brain Mapp 34(2):384–395. doi:10.1002/hbm.21437

Franz EA, Eliassen JC, Ivry RB, Gazzaniga MS (1996) Dissociation of spatial and temporal coupling in the bimanual movements of callosotomy patients. Psychol Sci 7(5):306–310. doi:10.1111/J.1467-9280.1996.Tb00379.X

Friston KJ, Frith CD, Liddle PF, Frackowiak RS (1993) Functional connectivity: the principal-component analysis of large (PET) data sets. J Cereb Blood Flow Metab 13(1):5–14

Gamboa OL, Tagliazucchi E, von Wegner F, Jurcoane A, Wahl M, Laufs H, Ziemann U (2014) Working memory performance of early MS patients correlates inversely with modularity increases in resting state functional connectivity networks. NeuroImage 94C:385–395. doi:10.1016/j.neuroimage.2013.12.008

Ge Y, Law M, Johnson G, Herbert J, Babb JS, Mannon LJ, Grossman RI (2004) Preferential occult injury of corpus callosum in multiple sclerosis measured by diffusion tensor imaging. J Magn Reson Imaging 20(1):1–7

Giorgio A, Portaccio E, Stromillo ML, Marino S, Zipoli V, Battaglini M, Blandino A, Bartolozzi ML, Siracusa G, Amato MP, De Stefano N (2010) Cortical functional reorganization and its relationship with brain structural damage in patients with benign multiple sclerosis. Mult Scler 16(11):1326–1334

Gooijers J, Swinnen SP (2014) Interactions between brain structure and behavior: the corpus callosum and bimanual coordination. Neurosci Biobehav Rev 43:1–19. doi:10.1016/J.Neubiorev.03.008

Gooijers J, Caeyenberghs K, Sisti HM, Geurts M, Heitger MH, Leemans A, Swinnen SP (2013) Diffusion tensor imaging metrics of the corpus callosum in relation to bimanual coordination: effect of task complexity and sensory feedback. Hum Brain Mapp 34(1):241–252. doi:10.1002/hbm.21429

Groppa S, Oliviero A, Eisen A, Quartarone A, Cohen LG, Mall V, Kaelin-Lang A, Mima T, Rossi S, Thickbroom GW, Rossini PM, Ziemann U, Valls-Sole J, Siebner HR (2012) A practical guide to diagnostic transcranial magnetic stimulation: report of an IFCN committee. Clin Neurophysiol 123(5):858–882

Harrison DM, Caffo BS, Shiee N, Farrell JA, Bazin PL, Farrell SK, Ratchford JN, Calabresi PA, Reich DS (2011) Longitudinal changes in diffusion tensor-based quantitative MRI in multiple sclerosis. Neurology 76(2):179–186

Hofer S, Frahm J (2006) Topography of the human corpus callosum revisited—comprehensive fiber tractography using diffusion tensor magnetic resonance imaging. NeuroImage 32(3):989–994

Hübers A, Orekhov Y, Ziemann U (2008) Interhemispheric motor inhibition: its role in controlling electromyographic mirror activity. Eur J Neurosci 28:364–371

Jeeves MA, Silver PH, Jacobson I (1988) Bimanual co-ordination in callosal agenesis and partial commissurotomy. Neuropsychologia 26(6):833–850

Jirsa VK, Fuchs A, Kelso JA (1998) Connecting cortical and behavioral dynamics: bimanual coordination. Neural Comput 10(8):2019–2045

Johansen-Berg H, Della-Maggiore V, Behrens TE, Smith SM, Paus T (2007) Integrity of white matter in the corpus callosum correlates with bimanual co-ordination skills. NeuroImage 36(Suppl 2):T16–T21

Kelso JA (1984) Phase transitions and critical behavior in human bimanual coordination. Am J Physiol 246(6 Pt 2):R1000–R1004

Kelso JA, Holt KG, Rubin P, Kugler PN (1981) Patterns of human interlimb coordination emerge from the properties of non-linear, limit cycle oscillatory processes: theory and data. J Mot Behav 13(4):226–261

Kennerley SW, Diedrichsen J, Hazeltine E, Semjen A, Ivry RB (2002) Callosotomy patients exhibit temporal uncoupling during continuous bimanual movements. Nat Neurosci 5(4):376–381

Kovacs AJ, Shea CH (2011) The learning of 90 degrees continuous relative phase with and without Lissajous feedback: external and internally generated bimanual coordination. Acta Psychol 136(3):311–320. doi:10.1016/j.actpsy.2010.12.004

Larson EB, Burnison DS, Brown WS (2002) Callosal function in multiple sclerosis: bimanual motor coordination. Cortex 38(2):201–214

Lazar M, Weinstein DM, Tsuruda JS, Hasan KM, Arfanakis K, Meyerand ME, Badie B, Rowley HA, Haughton V, Field A, Alexander AL (2003) White matter tractography using diffusion tensor deflection. Hum Brain Mapp 18(4):306–321

Mathiowetz V, Volland G, Kashman N, Weber K (1985) Adult norms for the Box and Block Test of manual dexterity. Am J Occup Ther 39(6):386–391

Meyer BU, Röricht S, Gräfin von Einsiedel H, Kruggel F, Weindl A (1995) Inhibitory and excitatory interhemispheric transfers between motor cortical areas in normal humans and patients with abnormalities of the corpus callosum. Brain 118(Pt 2):429–440

Mori S, van Zijl PC (2002) Fiber tracking: principles and strategies—a technical review. NMR Biomed 15(7–8):468–480

Muetzel RL, Collins PF, Mueller BA, M Schissel A, Lim KO, Luciana M (2008) The development of corpus callosum microstructure and associations with bimanual task performance in healthy adolescents. NeuroImage 39(4):1918–1925. doi:10.1016/j.neuroimage.2007.10.018

Nelson AJ, Hoque T, Gunraj C, Ni Z, Chen R (2009) Bi-directional interhemispheric inhibition during unimanual sustained contractions. BMC Neurosci 10(1):31

Netz J, Ziemann U, Hömberg V (1995) Hemispheric asymmetry of transcallosal inhibition in man. Exp Brain Res 104(3):527–533

Nimsky C, Ganslandt O, Fahlbusch R (2006) Implementation of fiber tract navigation. Neurosurgery 58(4 Suppl 2):ONS-292–ONS-303 (discussion ONS-303–ONS-294)

Oldfield RC (1971) The assessment and analysis of handedness: the Edinburgh inventory. Neuropsychologia 9(1):97–113

Pelletier J, Suchet L, Witjas T, Habib M, Guttmann CR, Salamon G, Lyon-Caen O, Cherif AA (2001) A longitudinal study of callosal atrophy and interhemispheric dysfunction in relapsing-remitting multiple sclerosis. Arch Neurol 58(1):105–111

Penner IK, Rausch M, Kappos L, Opwis K, Radu EW (2003) Analysis of impairment related functional architecture in MS patients during performance of different attention tasks. J Neurol 250(4):461–472

Pierpaoli C, Jezzard P, Basser PJ, Barnett A, Di Chiro G (1996) Diffusion tensor MR imaging of the human brain. Radiology 201(3):637–648

Pluim JP, Maintz JB, Viergever MA (2003) Mutual-information-based registration of medical images: a survey. IEEE Trans Med Imaging 22(8):986–1004. doi:10.1109/TMI.2003.815867

Polman CH, Reingold SC, Banwell B, Clanet M, Cohen JA, Filippi M, Fujihara K, Havrdova E, Hutchinson M, Kappos L, Lublin FD, Montalban X, O'Connor P, Sandberg-Wollheim M, Thompson AJ, Waubant E, Weinshenker B, Wolinsky JS (2011) Diagnostic criteria for multiple sclerosis: 2010 Revisions to the McDonald criteria. Ann Neurol 69(2):292–302

Preilowski BF (1972) Possible contribution of the anterior forebrain commissures to bilateral motor coordination. Neuropsychologia 10(3):267–277

Pulizzi A, Rovaris M, Judica E, Sormani MP, Martinelli V, Comi G, Filippi M (2007) Determinants of disability in multiple sclerosis at various disease stages: a multiparametric magnetic resonance study. Arch Neurol 64(8):1163–1168

Ranjeva JP, Pelletier J, Confort-Gouny S, Ibarrola D, Audoin B, Le Fur Y, Viout P, Cherif AA, Cozzone PJ (2003) MRI/MRS of corpus callosum in patients with clinically isolated syndrome suggestive of multiple sclerosis. Mult Scler 9(6):554–565

Rocca MA, Mezzapesa DM, Ghezzi A, Falini A, Martinelli V, Scotti G, Comi G, Filippi M (2005) A widespread pattern of cortical activations in patients at presentation with clinically isolated symptoms is associated with evolution to definite multiple sclerosis. Am J Neuroradiol 26(5):1136–1139

Rocca MA, Pagani E, Absinta M, Valsasina P, Falini A, Scotti G, Comi G, Filippi M (2007) Altered functional and structural connectivities in patients with MS: a 3-T study. Neurology 69(23):2136–2145

Rocca MA, Valsasina P, Absinta M, Riccitelli G, Rodegher ME, Misci P, Rossi P, Falini A, Comi G, Filippi M (2010) Default-mode network dysfunction and cognitive impairment in progressive MS. Neurology 74(16):1252–1259

Rossi S, Hallett M, Rossini PM, Pascual-Leone A (2009) Safety, ethical considerations, and application guidelines for the use of transcranial magnetic stimulation in clinical practice and research. Clin Neurophysiol 120(12):2008–2039

Rouiller EM, Babalian A, Kazennikov O, Moret V, Yu XH, Wiesendanger M (1994) Transcallosal connections of the distal forelimb representations of the primary and supplementary motor cortical areas in macaque monkeys. Exp Brain Res 102(2):227–243

Ruohonen J, Karhu J (2010) Navigated transcranial magnetic stimulation. Clin Neurophysiol 40(1):7–17. doi:10.1016/j.neucli.2010.01.006

Seitz R, Kleiser R, Butefisch C, Jorgens S, Neuhaus O, Hartung HP, Wittsack HJ, Sturm V, Hermann M (2004) Bimanual recoupling by visual cueing in callosal disconnection. Neurocase 10(4):316–325

Serbruyns L, Gooijers J, Caeyenberghs K, Meesen RL, Cuypers K, Sisti HM, Leemans A, Swinnen SP (2013) Bimanual motor deficits in older adults predicted by diffusion tensor imaging metrics of corpus callosum subregions. Brain Struct Funct. doi:10.1007/s00429-013-0654-z

Serrien DJ, Nirkko AC, Wiesendanger M (2001) Role of the corpus callosum in bimanual coordination: a comparison of patients with congenital and acquired callosal damage. Eur J Neurosci 14:1897–1905

Sigal T, Shmuel M, Mark D, Gil H, Anat A (2012) Diffusion tensor imaging of corpus callosum integrity in multiple sclerosis: correlation with disease variables. J Neuroimaging 22(1):33–37. doi:10.1111/j.1552-6569.2010.00556.x

Sisti HM, Geurts M, Gooijers J, Heitger MH, Caeyenberghs K, Beets IA, Serbruyns L, Leemans A, Swinnen SP (2012) Microstructural organization of corpus callosum projections to prefrontal cortex predicts bimanual motor learning. Learn Mem 19(8):351–357. doi:10.1101/lm.026534.112

Staffen W, Mair A, Zauner H, Unterrainer J, Niederhofer H, Kutzelnigg A, Ritter S, Golaszewski S, Iglseder B, Ladurner G (2002) Cognitive function and fMRI in patients with multiple sclerosis: evidence for compensatory cortical activation during an attention task. Brain 125(Pt 6):1275–1282

Stephan KM, Binkofski F, Halsband U, Dohle C, Wunderlich G, Schnitzler A, Tass P, Posse S, Herzog H, Sturm V, Zilles K, Seitz RJ, Freund H-J (1999) The role of ventral medial wall motor areas in bimanual co-ordination. Brain 122(2):351–368

Sullivan EV, Adalsteinsson E, Hedehus M, Ju C, Moseley M, Lim KO, Pfefferbaum A (2001) Equivalent disruption of regional white matter microstructure in ageing healthy men and women. NeuroReport 12(1):99–104

Swinnen SP (2002) Intermanual coordination: from behavioural principles to neural-network interactions. Nat Rev Neurosci 3(5):348–359

Tuller B, Kelso JA (1989) Environmentally-specified patterns of movement coordination in normal and split-brain subjects. Exp Brain Res 75(2):306–316

Vollmann H, Ragert P, Conde V, Villringer A, Classen J, Witte OW, Steele CJ (2014) Instrument specific use-dependent plasticity shapes the anatomical properties of the corpus callosum: a comparison between musicians and non-musicians. Front Behav Neurosci 8:245. doi:10.3389/fnbeh.2014.00245

Wahl M, Lauterbach-Soon B, Hattingen E, Jung P, Singer O, Volz S, Klein JC, Steinmetz H, Ziemann U (2007) Human motor corpus callosum: topography, somatotopy, and link between microstructure and function. J Neurosci 27(45):12132–12138

Wahl M, Hübers A, Lauterbach-Soon B, Hattingen E, Jung P, Cohen LG, Ziemann U (2011) Motor callosal disconnection in early relapsing-remitting multiple sclerosis. Hum Brain Mapp 32(6):846–855

Weinstein D, Kindlmann G, Lundberg E (1999) Tensorlines. Advection-diffusion based propagation through diffusion tensor fields. Paper presented at the proceedings of the conference on visualization

Weiss C, Nettekoven C, Rehme AK, Neuschmelting V, Eisenbeis A, Goldbrunner R, Grefkes C (2013) Mapping the hand, foot and face representations in the primary motor cortex—retest reliability of neuronavigated TMS versus functional MRI. NeuroImage 66:531–542. doi:10.1016/j.neuroimage.2012.10.046

Wittstock M, Grossmann A, Kunesch E, Walter U, Benecke R, Wolters A (2010) Altered callosal function in cerebral microangiopathy. J Neurol 257(4):590–597. doi:10.1007/s00415-009-5379-9

Yamanishi J, Kawato M, Suzuki R (1979) Studies on human finger tapping neural networks by phase transition curves. Biol Cybern 33(4):199–208

Yamanishi J, Kawato M, Suzuki R (1980) Two coupled oscillators as a model for the coordinated finger tapping by both hands. Biol Cybern 37(4):219–225

Yu CS, Lin FC, Liu Y, Duan Y, Lei H, Li KC (2008) Histogram analysis of diffusion measures in clinically isolated syndromes and relapsing-remitting multiple sclerosis. Eur J Radiol 68(2):328–334

Zaitsev M, Hennig J, Speck O (2004) Point spread function mapping with parallel imaging techniques and high acceleration factors: fast, robust, and flexible method for echo-planar imaging distortion correction. Magn Reson Med 52(5):1156–1166

Zarei M, Johansen-Berg H, Smith S, Ciccarelli O, Thompson AJ, Matthews PM (2006) Functional anatomy of interhemispheric cortical connections in the human brain. J Anat 209(3):311–320

Zito G, Luders E, Tomasevic L, Lupoi D, Toga AW, Thompson PM, Rossini PM, Filippi MM, Tecchio F (2014) Inter-hemispheric functional connectivity changes with corpus callosum morphology in multiple sclerosis. Neuroscience 266:47–55. doi:10.1016/j.neuroscience.2014.01.039